

PS Upscaling Fault Flow Properties for Evaluation of Cross-Fault Flow*

Alton A. Brown¹ and Russell K. Davies²

Search and Discovery Article #41390 (2014)**

Posted July 24, 2014

*Adapted from poster presentation given at 2014 AAPG Annual Convention and Exhibition, Houston, Texas, April 6-9, 2014

**AAPG©2014 Serial rights given by author. For all other rights contact author directly.

¹Consultant, Richardson, Texas, USA (altonabrown@yahoo.com)

²Rock Deformation Research USA, Inc., McKinney, Texas, USA

Abstract

An ongoing concern in flow modeling across faults is upscaling the fault-rock flow properties measured in the lab on cm-scale to the meter and tens of meter scale suitable for evaluating within-reservoir flow and exploration-scale sealing. It is proposed that upscaling is best accomplished by stochastic modeling of cross-fault flow guided by the geometries of fault-generated rock bodies (“geobodies”) as observed on outcrop. Preliminary models demonstrate that most resistance to flow transverse to the fault is in the low permeability fault rocks the fault core as opposed to the damage zone of deformation in the fault zone. Published and proprietary outcrop studies have demonstrated that the fault core is heterogeneous normal to the fault. Spatial correlation of lithology transverse to the fault core is on the order of mm to a cm, much too small to improve estimates of upscaled flow properties. Length of constituent bodies in the fault core can be traced along the fault on the scale of cm to meters in different settings. The fault core is best described as a composite of plate-shaped or equant geobodies with different permeabilities and seal capacities. Upscaling by numerical simulations of flow in composite rocks with these geometries can be compared to mathematical upscaling averages. Equant geobodies result in upscaled permeabilities very close to the geometric mean of the constituent geobody permeabilities and their volumes. Sealing depends on the relative size of the geobody relative to the width of the fault core. Plate-shaped geobody constituents lead to upscaled permeability between the harmonic and geometric means of the constituent geobody permeabilities, with upscale permeability approaching the geometric mean as the shape of the constituent geobody approaches equant. The thinner the geobody relative to the fault core width, the greater the seal capacity of the composite medium. Realistic upscaling of lab-measured permeability to real faults therefore depends on both the fractions of geobodies with different interpreted permeability and the likely geometry of the geobodies. Settings with smear and shearing of

ductile rocks lead towards platy fault core geometries, whereas settings where lenses or protolith is mixed into the fault core lead towards a more equant geobody shape.

Upscaling Fault Flow Properties for Evaluation of Cross-Fault Flow

Alton A. Brown, Consultant, Richardson, TX altonabrown@yahoo.com and Russell K. Davies, Rock Deformation Research USA, McKinney, TX

Abstract

An ongoing concern in flow modeling across faults is upscaling the fault-rock flow properties measured in the lab on cm-scale to the meter and tens of meter scale suitable for evaluating within-reservoir flow and exploration-scale sealing. It is proposed that upscaling is best accomplished by stochastic modeling of cross-fault flow guided by the geometries of fault-generated rock bodies ("geobodies") as observed on outcrop.

Preliminary models demonstrate that most resistance to flow transverse to the fault is in the low permeability fault rocks, the fault core, as opposed to the damage zone of deformation in the fault zone. Published and proprietary outcrop studies have demonstrated that the fault core is heterogeneous normal to the fault. Spatial correlation of lithology transverse to the fault core is on the order of mm to a cm, much too small to improve estimates of upscaled flow properties. Length of constituent bodies in the fault core can be traced along the fault on the scale of cm to meters in different settings.

The fault core is best described as a composite of plate-shaped or equant geobodies with different permeabilities and seal capacities. Upscaling by numerical simulations of flow in composite rocks with these geometries can be compared to mathematical upscaling averages. Equant geobodies result in upscaled permeabilities very close to the geometric mean of the constituent geobody permeabilities and their volumes. Sealing depends on the relative size of the geobody relative to the width of the fault core. Plate-shaped geobody constituents lead to upscaled permeability between the harmonic and geometric means of the constituent geobody permeabilities, with upscale permeability approaching the geometric mean as the shape of the constituent geobody approaches equant. The thinner the geobody relative to the fault core width, the greater the seal capacity of the composite medium.

Realistic upscaling of lab-measured permeability to real faults therefore depends on both the fractions of geobodies with different interpreted permeability and the likely geometry of the geobodies. Settings with smear and shearing of ductile rocks lead towards platy fault core geometries, whereas settings where lenses or protolith is mixed into the fault core lead towards a more equant geobody shape.

Terms

Protolith: undamaged rocks surrounding the fault from which fault rock is derived.
Fault rock: rock formed by any fault process such as smearing, mixing, shear, crushing, disaggregation, etc.
Damage zone: The zone of fault damage characterized by deformation bands, fractures, small-offset fault, etc. surrounding the fault core.
Fault core: zone of localized shear comprising a large fraction of total fault offset. Fault cores are typically zones with thick fault rock surrounding clasts or lenses of protolith and deformed protolith.
Geobody: non-genetic term for a body of rock characterized by relatively uniform properties. A fault core may be considered a geobody, but the fault core includes smaller geobodies representing the heterogeneity of the fault rock in the core.

Introduction

In most petroleum reservoir simulations, faults are modeled as surfaces separating offset columns of reservoir cells (Figure 1). Column-offset faults have no volume and no relative permeability. Flow near the fault is modified by two properties: transmissibility modifications across the fault plane (to mimic the flow resistance created by the fault) and modified linkages across the fault (to account for the offset of the fault; i.e., Manzocchi et al. 1999).

Representing faults by such simple geometry and properties hides the underlying lithological heterogeneity long recognized by structural geologists, reservoir geologists, and reservoir simulation engineers. Not only are most faults heterogeneous, the distribution and orientation of various lithological bodies within subsurface fault zones are not known due to limited imaging of faults in reservoirs. The problem for the reservoir geologist is assigning transmissibility modifications and cross-fault linkages to the modeled fault that causes the same fault flow behavior as that of the fault with its true lithological heterogeneity. This is a generalized upscaling problem (Farmer, 2002).

The magnitude of this upscaling is illustrated by comparing the volume of a typical fault-rock permeability sample against the typical volume of fault represented by the surface between cells in a reservoir simulation. Permeability samples have a volume of 1 - 10 m³. The volume of a fault 10 cm thick adjacent to a typical reservoir simulation cell 1 to 5 m thick by 25 - 50 m long is on the order of 10 million cm³ (Figure 2). Upscaling fault rock from lab sample volume to simulated reservoir volume is typically about a factor of a million to ten million. It would be very easy to upscale incorrectly without some sort of geological guidance. **The purpose of this poster is to provide this guidance.**

First, series flow theory is reviewed for to distinguish flow resistance caused by the fault from transmissibility changes incorporating both fault and protolith flow properties. The relative flow resistance of damage zone and fault core are then evaluated to show that the fault core accounts for most flow resistance caused by the fault where the fault core is fine grained and continuous on the scale of the reservoir cell.

The fabric and lithological fault core heterogeneity as seen on outcrop is then reviewed to develop general fault-core characteristics to be modeled. Single-phase flow was simulated across continuous fault cores with different heterogeneity to assess appropriate upscaling methods for fault cores with different geobody shapes. Upscaling of discontinuous fault core is then modeled to show that even a small fractional area open to flow around fault rock greatly reduces fault flow resistance below the fault-rock flow resistance. From these simulation results, a general approach to estimating fault flow resistance on the scale of reservoir cells is proposed.

Flow Resistance vs. Transmissibility

Single-phase transmissibility is calculated from the static model and used for flow calculations in most reservoir simulators. Transmissibility may be expressed in terms of dynamic or static characteristics:

$$T = \frac{Q\mu}{\Delta P} = \frac{Ak}{\Delta L}$$

Single-phase transmissibility:

where Q: volumetric flux; μ : viscosity; ΔP : pressure difference between cells; A: area of contact between cells; k: permeability; ΔL : flow length between cell centers.

Properties of upscaled cells are different, so transmissibility is calculated from the average of cell properties. Flow between adjacent cells is always series flow (Figure 3). In series flow problems, flow resistance (L/k) and flow resistivity (L/k) are more convenient, because flow resistance is additive in series flow. The total matrix flow resistance (R_m) is $R^1 + R^2 = L^1/k^1 + L^2/k^2$. Flow modification by adding a fault is simply adding an additional resistance term (Figure 3B). Units of flow resistance used here are meters per millidarcy.

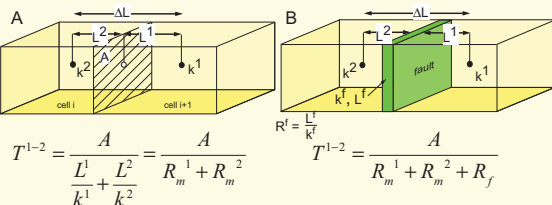


Figure 3. Transmissibility between adjacent cells. (A) without a fault, (b) with a fault. The fault flow resistance (R_f) is completely independent from properties of adjacent cells. R_f contains effects of both upscaled permeability and width, thereby simplifying upscaling in the presence of fault width and permeability variations. Transmissibility between cells separated by a fault is simply calculated by dividing the total flow area between cells by the sum of the resistances of the cells and the fault.

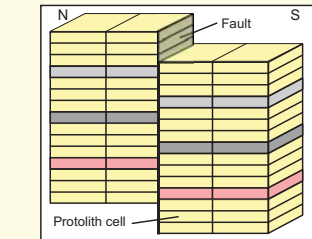


Figure 1. Simulator scale model of simple column-offset fault. The fault has no volume; it has modified cell linkages and transmissibilities. In the default case, cell links across the fault proportional to their contact area. The assumed properties of the upscaled fault are used to modify the transmissibility across the fault surface.

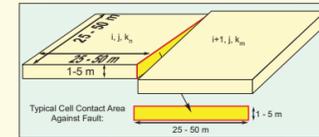


Figure 2. The large size of typical reservoir simulation cells cause column-offset faults in simulations to represent a fault rock volume on the order of 25 to 250 m³, assuming fault rock about 10 cm thick.

Where in a Fault is Most Flow Resistance?

Summary

The main control on total fault-flow resistance is the presence, permeability, and continuity of the fault core. Where it is relatively continuous and impermeable, the fault core dominates total fault-flow resistance and damage-zone properties can be ignored.

In this presentation, we consider the damage zone comprising deformation features with permeability lower than that of the reservoir. Deformation bands are a common damage zone deformation style in porous reservoir sandstones and, with adequate mean effective stress, have a reduced permeability across the bands. If resistive elements in the damage zone such as deformation bands are linked to form continuous low-permeability bodies, the damage-zone flow resistance can be significantly reduced.

Where the faults cut clay-rich layers, they incorporate the clay into their fault core and create a low permeability fault rock. If the fault core has the permeability equal or less than that of the deformation bands, its greater cumulative thickness concentrates most flow resistance in the core. Where the fault core has significantly greater flow resistance than the damage zone, cross-fault flow resistance interpretation can be simplified to analysis of the fault core rather than considering both the fault core and the damage zone. This can greatly simplify the problem of evaluating and upscaling cross-fault flow resistance.

Fault Flow Resistance: Damage Zone vs. Fault Core

We evaluate the distribution of flow resistance across a fault with a typical damage zone of deformation bands and a low permeability fault core. To evaluate the maximum possible flow resistance, both damage zone and fault core are assumed to be continuous normal to flow on the scale of investigation. Flow across continuous, homogeneous layers is series flow. Series flow resistance is the sum of the flow resistance of the component layers. The assumption of series flow gives the maximum potential flow resistance of a complex medium.

The lower part of Figure 4 shows the idealized fault cross section from which cumulative flow resistance was calculated. Permeabilities of lithologies are shown at base of the figure. An outer damage zone comprising protolith with approximately 10 deformation bands per meter is 3 m wide left of the fault and 1.5 m wide right of the fault. Width of individual deformation bands is 1 mm, giving a cumulative deformation band width of 4.5 cm. An inner damage zone comprising protolith deformed to reduce its permeability by a factor of 100 is 0.5 m thick on each side of the fault core. The fault core is 15 cm wide.

To illustrate the contribution of different layers to the total flow resistance, the cumulative flow resistance is plotted as a function of position along the flow length with assumed flow from left to right (upper part of Figure 4). Fault core flow resistance is about 96% of the total resistance of 156 m/mD. Total damage-zone flow resistance is about 6 m/mD, roughly equivalent to replacing the damaged rock by 0.75 mD rock with the same width. Inner damage zone flow resistance is negligible (0.7% of total). The modeled flow resistance across the fault is about 2600 times greater than the flow resistance of protolith with the same flow path length.

In the model shown on Figure 4, incorporating permeability and spacing for deformation bands within the range of published values (e.g., Solum et al. 2010), cannot increase the damage-zone flow resistance to the flow resistance calculated for this fault core. It is difficult to make a damage zone cross-fault flow resistance using realistic deformation band permeabilities, width and spacing equal to that of a fault core that has fault rocks with typical permeability and width for high-clay fault rock.

Is Fault Flow Resistance Significant?

Where fault flow resistance is a small fraction of the flow resistance between reservoir cells juxtaposed by the fault, its transmissibility multiplier of effectively 1 (the default value). If the magnitude of expected fault flow resistance relative to protolith flow resistance can be estimated early on, fault segments with negligible flow resistance can be identified and ignored so that time is spent evaluating faults with greater potential for modifying reservoir flow.

Such a screening step requires an estimate of reservoir protolith flow resistance between cells juxtaposed by the fault. This is a series flow problem. Where reservoir facies are juxtaposed against non-reservoir facies, the between-cell flow resistance is much higher than between two reservoir cells. The flow resistance added by the fault rock is almost certainly negligible compared flow resistance of reservoir juxtaposition against a non-reservoir cell.

For reservoir-reservoir juxtaposition, between-average permeability can be used as a guide to estimating between-cell flow resistance. Figure 7 plots between-cell reservoir flow resistance (vertical axis) as a function of average reservoir permeability (horizontal axis) and distance between juxtaposed cell centers (lines).

With typical between-cell flow lengths of 50 to 100 m and typical reservoir (protolith) permeability in the 10 to 1000 mD range, protolith flow resistance is on the order of 0.05 to 10 m/mD. Even faults with low flow resistance become important in permeable reservoirs, whereas fault with similar low flow resistance would add negligible flow resistance to juxtaposed tight reservoir cells.

In the previous example (above), fault core and damage zone fault flow resistances are 150 and 6 m/mD, respectively. Both fault core and damage zone (in the absence of a continuous fault core) would add significant flow resistance to typical reservoir cells and would have to be incorporated in the reservoir simulation.

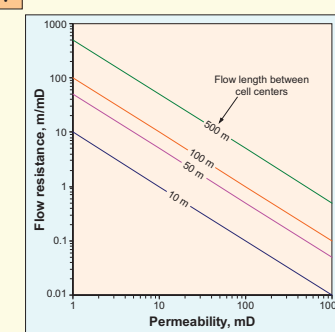


Figure 7. Protolith flow resistance as a function of cell size (distance between cell centers) and permeability. See discussion to left.

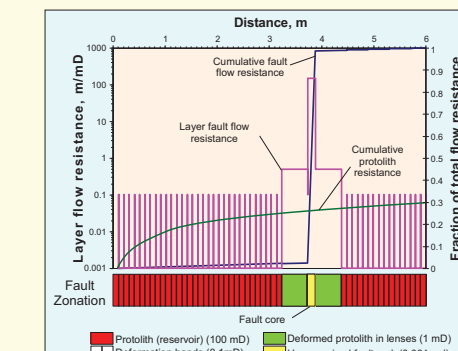


Figure 4. Incremental and cumulative flow resistance across a fault consisting of an outer damage zone with deformation bands, an inner damage zone of deformed protolith, and an argillaceous fault core. Flow resistance is in units of m/mD. Lithology permeabilities are shown at bottom.

Geometry of Fault Cores

Results presented in the previous section demonstrate that the fault core is responsible for most flow resistance where the fault core is continuous and has low permeability. We will now examine outcrop faults to better understand the fabric of fault cores where they are continuous.

Humur A fault, Wadi al Humur, western Sinai, Egypt

The Humur fault system is part of the eastern Gulf of Suez Rift (Tueckmantel et al. 2010). The Humur A fault cuts Early Cretaceous Malha Formation siliciclastics with approximately 100 m normal displacement of middle Cenozoic age (Lickorish and Tueckmantel, 2008). The fault has a relatively narrow damage zone and moderately thick fault core (Figure 8). Fault core comprises fine sand, silt, and mudrock layers parallel to the fault, each a few cm thick. Some fault rock layers are homogeneous; other layers are composite with irregular clasts of sandstone in a more continuous matrix of finer-grained fault rock. Most layers extend the length of the outcrop (~1 m).

Baba "B" Fault, Wadi Baba, western Sinai, Egypt

The Baba fault is a basement-involved fault forming part of the eastern Gulf of Suez Rift (Tueckmantel et al. 2010). Baba "B" fault is a strand of the Baba fault zone with normal offset. Limestones and dolomites of the Carboniferous Umm Bagma Formation (hanging wall) are juxtaposed against Cambrian Araba Formation sandstones (footwall) with stratigraphic offset of about 13 m near the base of the outcrop (Lickorish and Tueckmantel, 2007). The damage zone is relatively wide (5 - 8 m) with numerous small faults and rotated protolith blocks. The fault core comprises clay smears, sand smears, and fault gouge forming a zone up to 30 cm thick with a few large sandstone lenses. Lenses have long axes parallel to the fault plane (Figure 9). Clay smear thin near the thicker lenses and near the base of a thick sandstone unit in the upper Araba Formation in the footwall. Away from the lenses, the fault core is layered parallel to the fault, with layers of more pure clay smear alternating with fault rock (?) layers with smaller clasts of sandstone protolith (Figure 9).



Figure 9. Lower part of B strand of the Baba fault exposed in Wadi Baba. Fault core is labeled. Figure courtesy of Christian Tueckmantel.

Salina Creek Fault, Salina Canyon, Sevier County, Utah

The Salina Creek fault is an informal name for a minor fault in the Water Hollow Fault zone exposed in a tunnel about 20 km east of Salina, Utah (Covault 2006). The fault cuts the thick-bedded Cretaceous Castlegate Sandstone with normal offset of about 8 m. The Castlegate Sandstone comprises thick bedded sandstones with thin argillaceous sandstones and impure mudrocks. The fault has a probable age of Middle Miocene to Pre-Pleistocene.

Fault damage zone comprises small faults, deformation bands, and bed rotation. The fault core comprises sheets of fault rock oriented parallel to the fault. Fault rock layers are poorly consolidated mud smears, sand smears, and gouge (Figure 10). Gouge has small sandstone clasts and muddy matrix.

Generalized Fault Core Fabric

These examples and many other faults with fault cores developed in sedimentary protoliths show similar characteristics (Figure 11).

- Fault cores are not a homogeneous, even on the cm scale. Cores of faults through sedimentary rocks typically have a layered fabric.
- Layers are platy geobodies oriented parallel or nearly parallel to the fault, discontinuous to continuous on the scale of the outcrop (tens of cm to meters).
- Some platy geobodies have a relatively homogeneous internal fabric due to their origin by smearing or due to complete homogenization by shear.
- Others platy geobodies are heterogeneous with clasts or lenses of altered protolith in a finer-grained fault-rock matrix. The continuous medium ("matrix") surrounding clasts and lenses typically has lower permeability than the clasts and lenses due to the higher shear and/or higher clay content in the matrix. Heterogeneity is sufficient for the fault core to be described as random anisotropic medium.
- Spatial correlation length does not exceed the size of the geobody. Spatial correlation normal to the fault is on the order of a cm or less to several cm. Spatial correlation along the fault is on the order of tens of cm to meters. Spatial correlation lengths are so much less than the lengths of reservoir simulator cell edges that upscaling problems can treat permeability variations between geobodies as randomly distributed.

For further discussion of fault fabrics, please see the poster by Davies et al. (2014) in this AAPG poster session, booth xx.



Figure 8. Humur A fault, Section 3. Fault core is about 20 cm thick, with distinctly layered fabric. Figure from RDR 2008 Fault Foundation Report. Figure courtesy of Christian Tueckmantel.

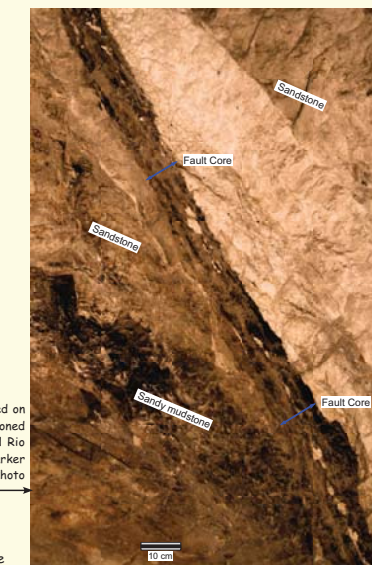


Figure 10. Salina Creek fault exposed on the north wall of Tunnel #4 of the abandoned Castle Valley Branch of the Denver and Rio Grande Railroad. Fault core is labeled. Darker colored lithologies are more clay-prone. Photo by Russell Davies.

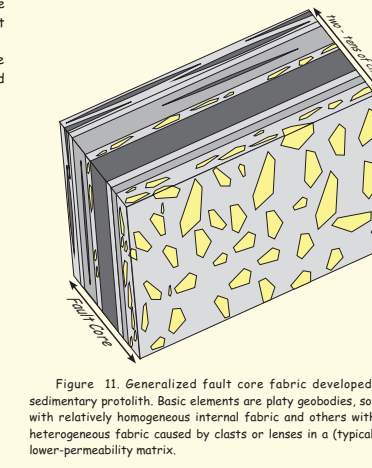


Figure 11. Generalized fault core fabric developed in sedimentary protolith. Basic elements are platy geobodies, some with relatively homogeneous internal fabric and others with a heterogeneous fabric caused by clasts or lenses in a (typically) lower-permeability matrix.

Upscaling Model

Fault outcrops demonstrate that fault cores continuous on the outcrop scale in sedimentary protoliths are heterogeneous across the fault as well as along the fault. Upscaling requires consideration of small-scale permeability variation in all directions.

We modeled how the shape of geobodies within the fault core and the underlying permeability distribution assigned to the fault rock affects upscaled single-phase flow. Details of the model are discussed below. Results are on the next panel.

Upscaling Model Description

Models address the effects of the assumed permeability distribution and the shape of geobodies (cells) comprising the fault rock. All simulations model flow through a homogeneous reservoir with a single, continuous but heterogeneous fault rock barrier. The total model volume is much less than the volume of fault rock represented by a cell edge in a reservoir simulation, but model permeability variation is on the scale observed on outcrop.

Two distributions of fault rock permeability are assigned: an equal, lognormal distribution and a truncated lognormal distribution. Fault elements are given either equant or platy shapes. Platy fault elements are flattened parallel to the fault. A model consists of a cell shape and a fault-rock permeability distribution. Six realizations of each model were run.

Fault rock permeability is upscaled using the pressure-solver approach for single-phase (water) flow. Flow is simulated using the Plano Research FlowSim reservoir simulator in single-phase (aqueous) mode. Upscaled permeability is estimated from pressure distribution and flow rate after 1000 days of simulated flow.

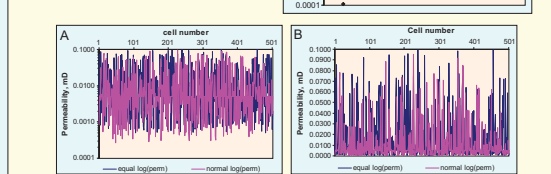
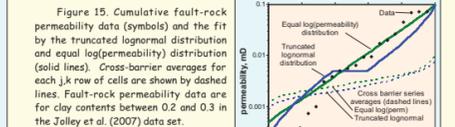


Figure 16. Realization 1 permeabilities assigned to each of the first 500 of 3000 cells comprising the fault rock, displayed on a logarithmic (A) and linear (B) permeability scale.

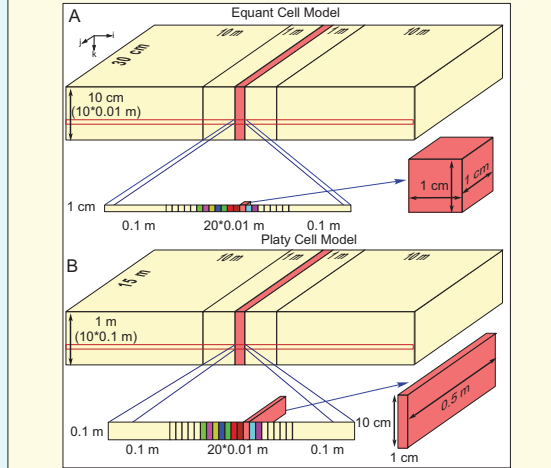


Figure 17. Gridding for random equant (upper) and platy (lower) cells in model. Fault-rock comprises the center 10 i cells in the center of the model. Fault rock has random permeability assignments but protolith has a uniform permeability of 100 mD.

Upscaling Fault Flow Properties for Evaluation of Cross-Fault Flow

Alton A. Brown, Consultant, Richardson, TX altonabrown@yahoo.com and Russell K. Davies, Rock Deformation Research USA, McKinney, TX

Effects of Permeability Distribution and Geobody Shape on Upscaled Cross-fault Flow

Effects of Underlying Permeability Distribution

The two permeability distributions modeled in this study (equal log(permeability) and truncated lognormal permeability) are discussed on the previous panel. The permeability upscaled from the equal log(permeability) distribution is about 20% higher than that upscaled from the truncated lognormal permeability distribution (Figure 12). This is caused by differences in averages of each permeability distribution (Figure 12). Effects of the assumed permeability distribution are factored out if upscaled permeability is compared to permeability averages.

Both permeability distributions have exceptionally large variance (Figure 15). Distribution variance is reduced significantly by averaging permeability in each cross-fault row of cells. Models with the same permeability distribution and fault-element shape have an even lower upscaled permeability variance. Upscaled permeabilities lie within about 5% of each other (Figures 12, 13). This is a direct consequence of the averaging process that is fundamental to upscaling. The average of a sample size in the thousands will converge on the population mean despite the high variance of the population.

Effects of Fault Geobody Shape

The fault has the same geometry in all realizations, but the shape of geobodies within the faults are either platy or equant, as described in the previous panel. Geobody shape significantly affects upscaled permeability. Upscaled permeability of fault rock with equant cell shape is very close to the geometric average of the fault-rock permeabilities (Figure 13A). Upscaled fault permeability of faults with platy geobodies lie between the harmonic and geometric averages of the cell permeabilities (Figure 13B). Fault geobodies extending across the entire model have pure series flow, so permeability upscalings to the harmonic average.

Means with values between geometric and harmonic means can be evaluated using the generalized power mean:

$$M_p = \left(\frac{1}{n} \sum_{i=1}^n x_i^p \right)^{1/p}$$

Geometric and harmonic means correspond to p values of 0 and -1, respectively, in the power mean equation. Aspect ratios of equant and infinite platy cells are 1 and zero, respectively. Upscaled permeabilities of fault rock with constituent platy cells with the 0.1 minimum aspect ratio modeled here are fit with a p value near -0.6 (Figure 13B). The p value can be approximated from the aspect ratio of the cells using the following relationship: p = (aspect ratio)^{0.5}-1. This relationship needs to be verified by additional modeling.

Upscaled Seal Capacity

Seal capacity can be expressed by the pore-throat diameter at the threshold pressure (Katz and Thompson 1987). The throat diameter is proportional to the square root of permeability (Katz and Thompson 1987). This means that permeability can be used to judge relative seal capacity, where lower permeability has higher seal capacity. Seal capacity of each realization is estimated by first identifying the tightest seal in each row across the heterogeneous fault rock, and then identifying which of these rows has the lowest seal capacity. The seal capacity along each j,k row of fault core cells is that of the cell with the minimum permeability. The seal capacity for the entire fault core is the seal capacity of the j,k row with the weakest seal (highest permeability). Calculated seal capacity (in terms of permeability) corresponds approximately to the geometric mean of the permeabilities for that realization. Unlike upscaled permeability, the seal capacity shows significant variation between realizations. This is caused by the process of selection: permeability is upscaled by averaging; upscaled seal capacity is estimated using minimum and maximum functions.

Figure 14. Upscaled seal capacity for the six realizations of the two permeability distributions. Seal capacity is shown in units of permeability (see text). Lowest permeability corresponds to highest seal capacity. "E" = equal log(permeability) distribution. "L" = truncated lognormal permeability distribution.

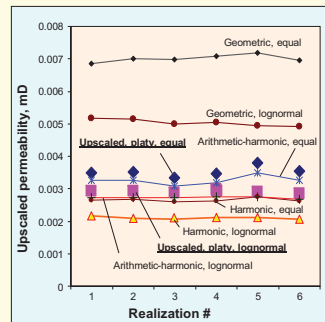


Figure 12. Comparison of pressure-solver upscaled permeability to averages for the permeability distributions assuming platy geobodies. "lognormal" = truncated lognormal permeability distribution; "equal" = equal log(permeability) distribution. "geometric, harmonic, etc." refer to means calculated directly from cell permeabilities.

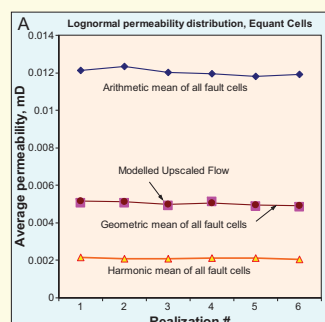
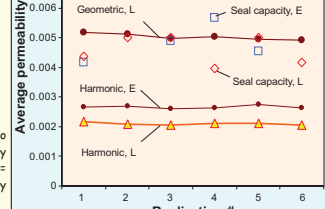
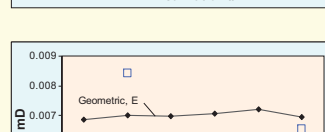
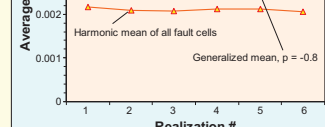


Figure 13. Power-solver upscaled permeability compared to different means for equant (A) and platy (B) cell shapes using truncated lognormal permeability distribution. Six realizations are shown for each. Results are similar for the equal log(permeability) distribution.



Fault Core Continuity

Previous discussion concerned flow across faults with continuous fault core with different constituent geobody shape. We now evaluate upscaled fault flow resistance where there is a discontinuity (hole) through the fault, so that flow can go around as well as through the fault rock.

As before, we investigate this problem with numerical flow simulations. For simplicity of interpretation, faults will be modeled as homogeneous, isotropic barriers, each with a single hole of varying size that connects the reservoir cells on either side of the fault barrier.

Model

The barrier has a fixed width of 10 cm (10 layers 1 cm wide). Barrier cells are populated with either a uniform fault-rock permeability or a uniform reservoir permeability of 100 mD in all models. Two fault-rock permeabilities are used in different models, 0.1 mD (barrier flow resistance of 1 m/mD) and 0.0001 mD (barrier flow resistance of 1000 m/mD). These simulate weak and strong fault core barriers, respectively. Gridding is shown in Figure 18. The hole size is the fraction of the barrier cells that are assigned reservoir permeability. Different model realizations evaluate different hole areas.

Flow is simulated using the Plano Research FlowSim reservoir simulator in single-phase (aqueous) mode. Model flow resistance is calculated from pressure distribution and flow rates after 1000 days of simulated flow. Upscaled fault-low resistance is the model flow resistance minus the flow resistance where all barrier cells assigned a reservoir permeability.

Results

Upscaled fault flow resistance is low (<0.05 m/mD) in all simulations with over 77% of the fault area open to reservoir-reservoir juxtaposition (Figure 19). Fault flow resistance approximately equals model reservoir flow resistance of 0.12 m/mD where the hole area comprises about 4% of the fault area. Only where the open area is

about 1% or less of the total model cross section area does the flow resistance of the fault approach the flow resistance of the fault rock. Upscaled fault flow resistance of this discontinuous fault core is approximately the harmonic average of the fault rock and reservoir flow resistance in the fault zone (weighted by their volumes in the fault zone), multiplied by a tortuosity of about 4.

The flow resistance of models with strong fault barriers is similar to that of weak barriers until open flow area is less than about 5%. Where flow resistance of the weak barrier equals that of the strong barrier, the fault rock flow resistance does not significantly contribute to the overall fault flow resistance. Upscaled fault-flow resistance is caused by reduced high-permeability cross-sectional area through the fault zone and increased flow path tortuosity. Flow follows paths of least resistance. Even an exceptionally narrow pathway with high permeability gives less flow resistance than substantially wider flow paths with low permeability.

Implications

Flow resistance by a discontinuous fault barrier is controlled mainly by the resistance of flow through holes or bypass systems through or around the fault barrier until the fault barrier is almost completely closed. For modeled conditions, reservoir transmissibility is reduced by half where the fault barrier covers about 96% of the model flow area. The upscaled fault flow resistance is much greater than the flow resistance of the fault rock until about 99% of the modeled flow system is closed by the fault rock. **Flow across a fault with a discontinuous fault core is controlled less by fault-rock permeability and fault width than by the continuity of the fault core.** No matter how well characterized the fault-rock permeability and width, it will not represent the flow resistance of the upscaled fault unless the fault core is almost completely continuous across the area of interest.

These simulations consider fault core and unaltered protolith only for simplicity. In real faults with damage zones, cross-fault flow at fault core discontinuities will be controlled by the flow resistance of the damage zone in the vicinity of the fault core discontinuities rather than the protolith.

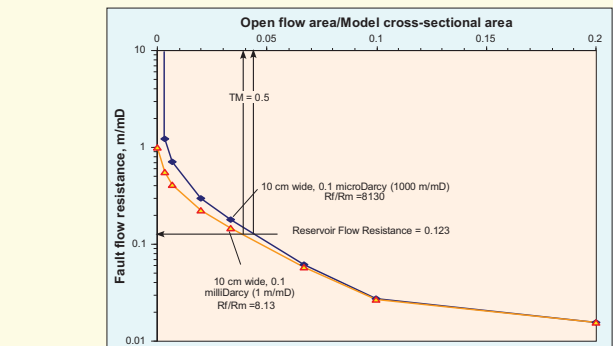
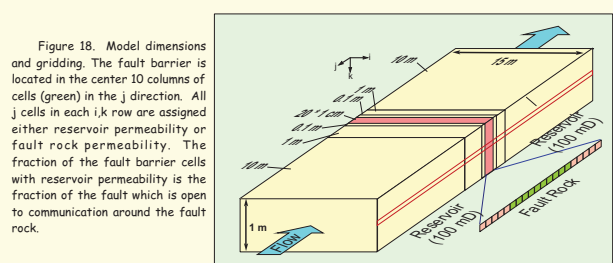


Figure 19. Fault-core flow resistance as a function of the fraction of the model area that bypasses the fault. Results are shown for two fault-flow resistances representing strong (highly resistive) and weak (low resistance) flow barriers. The fraction open flow area corresponding to

Upscaling Faults with Discontinuous Core

The upscaled flow resistance of a fault with a discontinuous core can be evaluated from the presence or absence of a discontinuity (hole) over the area of interest that exceeds some critical size in the fault core. If a hole is present, the flow resistance is upscaled from the hole size, and the flow resistances of the core, and the damage zone.

Where holes are small or absent, upscaled fault flow resistance is that of the fault core (core width divided by permeability). Where holes exceeding the critical size are present, upscaled flow resistance is the harmonic average of the hole fractional area divided by the flow resistance of the damage zone and the fault rock area (one minus hole fractional area) divided by the flow resistance of the fault rock. This quantity is multiplied by some tortuosity which will probably be in the range of 3 - 6. Unless damage-zone flow resistance is high, flow resistance of the upscaled fault is quite low for hole fractional areas greater than about 5% of the total fault area. The problems for fault upscaling are therefore (1) estimating the likelihood of the presence of a hole in a given area and, if present, (2) estimating the fraction of the total fault area occupied by the hole.

The first problem (presence of a hole) is a Poisson sampling problem. Assume that there is an average number of holes through a fault core per unit area of the fault for a given SGR or architecture. This hole frequency can be determined from the fraction of open fault area and the average hole size (Figure 20). The likelihood of no hole, one hole, etc. being absent within a fault area the size of a reservoir cell is determined by the Poisson distribution.

For example, assume that there are 0.01 circular holes/m² of fault area (one hole per 100 square meters), an average hole size is 0.5 m² area (0.8 m diameter), and an area of the fault of interest between two cells is 100 square meters. The Poisson statistic predicts that the fault between the two cells will have no holes in approximately 37% of realizations. These realizations would be assigned the upscaled fault-core flow resistance because fluids must flow through the fault core. Another 37% of realizations would have a single hole, giving a fraction of open flow equal to 0.5/100 or 0.005 m²/m². For the previous model (Figure 19), these cells would have a fault resistance near 0.5 m/mD, and the flow resistance would be somewhat affected by the flow resistance of the fault core. Another 18% of cell realizations would have two holes, giving an area open to flow of about 1% and flow resistance near 0.25 m/mD. The remaining 8% of cell realizations would have three or more holes and a flow resistance of 0.2 m/mD or less. Flow resistance of realizations with two or more holes are independent from the flow resistance of the fault core and controlled entirely by flow resistance of the damage zone if present.

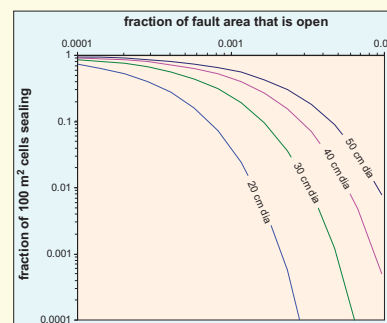


Figure 20. Fraction of cells with 100 m² contact area with a fault that are sealing (lock holes in the fault core) as a function of the fraction of the fault surface that is open and the modeled hole size.

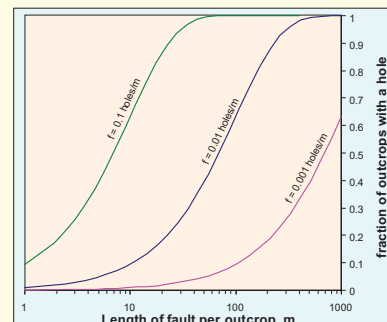


Figure 21. Fraction of outcrops with an exposed hole as a function of exposed fault lengths and hole frequency.

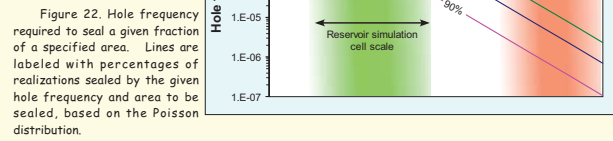


Figure 22. Hole frequency required to seal a given fraction of a specified area. Lines are labeled with percentages of realizations sealed by the given hole frequency and area to be sealed, based on the Poisson distribution.

Discussion and Implications

Upscaling approaches and results are a bit different from those used in other studies. These differences result from different conceptualization of fault architecture. We distinguish upscaled fault-rock permeability from upscaled fault permeability. We recognize that SGR and other clay content indices may directly control upscaled fault rock permeability, but SGR controls on upscaled fault permeability can be indirect. Upscaled fault permeability is controlled by the fault architecture and especially the continuity of the fault core. Where fault core is continuous, fault-rock flow resistance approximates the overall fault flow resistance; where fault cores have holes or discontinuities, fault flow resistance is controlled by the size of the holes and damage-zone flow resistance.

Upscaled Fault-Rock Permeability

Results presented here show that upscaling from sample to simulator-sized cells averages between the geometric and the harmonic means, and the constituent geobody shape controls where between these means the upscaled permeability lies. For typical aspect ratios of fault core elements, upscaling follows the power mean with a p value near -0.6 to -0.8.

These results directly contradict the results of Manzocchi et al. (1999), who conclude that upscaling follows an arithmetic average with minor modifications for effects of pressure gradient difference in low permeability reservoirs. Harmonic and arithmetic upscaling can differ by orders of magnitude; these differences are not trivial.

Different upscaling results are a direct consequence of how heterogeneity within the fault is conceptualized (Figure 22). Manzocchi et al. (1999) assume that fault rock is homogeneous normal to the fault plane and heterogeneous parallel to the fault plane. Upscaled fault-rock models in this poster assume heterogeneity on the scale of the laboratory samples both normal and parallel to the fault plane. Fault-rock heterogeneity in all directions is more consistent with outcrop observations.

Heterogeneity of Upscaled Fault Rock

As shown by Figure 13, small-scale permeability heterogeneity averages out where upscaling by factors of thousands or more. Fault rock upscaled from the same underlying sample permeability population to the size of the edges of reservoir simulation cells will have similar flow resistance. The permeability heterogeneity measured in sample populations with similar clay content cannot be used to characterize the heterogeneity of the upscaled fault rock or the upscaled fault. Heterogeneity of upscaled faults is controlled by the fabric, especially the continuity of the fault core as discussed below.

Controls on Upscaled Fault Flow Resistance

The method for upscaling fault flow resistance depends on whether the fault core is continuous on the scale of interest (Figure 23). Where the fault core is continuous, the upscaled fault flow resistance is the expected fault-core width divided by the power mean of the calibration sample permeabilities with a p value controlled by the fabric within the fault core. Fault core with an isotropic fabric has P value close to zero (geometric average). Fault core with a platy fabric has P values close to -0.6. If the fault core is continuous, upscaled fault flow resistance in cells with similar environmental parameters such as SGR are likely to be similar, so heterogeneity is based on uncertainty in average SGR and fault width rather than the spread of the constituent permeability measurements.

Where the fault core is discontinuous, the frequency of holes and size of holes controls upscaled flow resistance, because fluids flow around tight fault rock. Upscaled fault flow resistance is the harmonic average of the fault-core and damage-zone flow resistance weighted by area of hole (for damage zone) and multiplied by a suitable tortuosity (between 3 and 6, depending on permeability difference). Upscaled fault flow resistance heterogeneity can be estimated from the Poisson distribution.

Implications of Upscaling Models

The generalized upscaling work flow proposed here has a number of consequences, many of which have not been completely evaluated:

- Where the fault core is discontinuous across the area to be upscaled, SGR does not directly control fault flow resistance. SGR might control upscaled fault flow resistance indirectly. For example, interbedded sandstones and mudrocks which lead to higher SGR are also characterized by a higher mechanical heterogeneity that may control the discontinuity of the fault core and damage zone.
- Where the fault core is discontinuous but damage features form a continuous linked barrier, the flow resistance of the damage zone controls fault flow resistance. However, the same sort of continuity arguments apply to damage-zone flow resistance. If damage features are discontinuous and do not form continuous surfaces with high flow resistance, fluids will flow around deformation features and fault flow resistance may be negligible.
- Outcrop data are too sparse to directly calibrate the size and density of holes through the fault core. Instead, outcrops can be used to calibrate mechanical models of fault architecture. Size and distribution of holes developed in modeled faults might then be used to evaluate the hole density and geometry in fault cores developed in similar stratigraphic sequences under similar stress settings.
- Capillary (membrane) sealing by the fault is low unless the fault core is continuous and has low permeability. Where the fault rock is continuous, the threshold pressure can be approximated from the measured calibration permeabilities using a geometric averaging approach discussed with Figure 14.

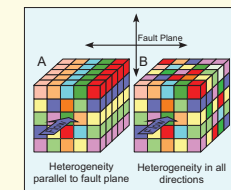


Figure 22. Fault core heterogeneity concepts. (A) Heterogeneity to the fault plane leads to upscaling by arithmetic average of cell permeabilities. (B) Heterogeneity in all directions leads to geometric to harmonic averaging of cell permeabilities, depending on cell aspect ratios.

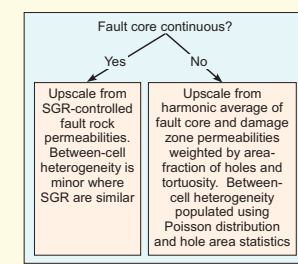


Figure 23. Summary flow diagram for evaluating upscaled cross-fault flow resistance based on models run in this study.

Conclusions

- Simple models show that the flow resistance of a low permeability fault core continuous on the scale of interest far exceeds the flow resistance by the damage zone (Panel 1). If fault cores are continuous, damage zone architecture has little effect on the overall fault flow resistance. The key issue for cross-fault flow upscaling is determining continuity of the fault core.
- Fault cores are heterogeneous both along and normal to the fault (Panel 1). Fault cores are typically composed of geobodies with equant to platy shapes aligned almost parallel to the fault plane. Upscaling fault core flow resistance from lab sample size to reservoir-simulation scale must include heterogeneity across the fault core as well as along the fault core. Such models must also consider the shape of the constituent geobodies.
- Upscaled permeabilities for fault cores heterogeneous both normal and parallel to the fault plane follow the power mean between the geometric and the harmonic average of the permeability of the constituent elements.
- The shape of constituent geobodies influences the upscaled permeability. Fault cores with equant geobodies upscale to geometric averages of the permeabilities of the constituent geobodies. Fault cores with platy geobodies upscale to power means with p values near -0.6. Specifically, the p exponent in the generalized power-mean equation can be related to the ratio of geobody length parallel to flow to the minimum length orthogonal to flow (aspect ratio) by the following relationship: p = (aspect ratio)^{0.5} - 1.
- Although fault-rock permeability distributions have high variance typically extending over several orders of magnitude, the permeabilities upscaled from different realizations of the same high-variance population have low upscaled permeability variance (within 5% of each other). The variance of the underlying permeability distribution cannot be used to stochastically distribute upscaled permeabilities.
- Flow can completely bypass the upscaled fault core where the fault core is discontinuous. Upscaled flow through faults with discontinuous cores only approach the upscaled fault rock flow resistance where less than 1% of fault area bypasses fault core. The major control for upscaling in faults with discontinuous fault core is not upscaling fault-rock permeability; it is estimating the frequency and size of the holes in the fault.
- Presence of a hole in a fault in a given fault area is a Poisson sampling problem. Poisson statistics can be used to upscale fault-flow in different realizations. However, determining the hole frequency necessary to apply this approach is difficult due to the relatively limited lengths of faults exposed on most outcrops.

References

Covault, A. H., 2006, Structural Architecture and Deformation of the Salina Creek Tunnel Normal Fault Zone, Central Utah, USA: Masters Thesis, University of Texas at Dallas, 112 p.

Davies, R., R. Knipe, M. Welch, H. Lickerish, D. Povey, and A. Brown, 2014, Fault Zone Complexity: Impact on Seal Analysis and Prediction (poster): AAPG Annual Convention, April 2014, Houston, TX.

Farmer, C. L., 2002, Upscaling: a review: International Journal for Numerical Methods in Fluids, v. 40 p. 63-78.

Freeman, C. L., S. D. Harris, and R. J. Knipe, 2008, Fault seal mapping - incorporating geometric and property uncertainty, in: Robinson, A., Griffiths, P., Price, S., Hegre, J. and Mugeridge, A. (eds) The Future of Geological Modelling in Hydrocarbon Development, The Geological Society, London, Special Publications, v. 309, p. 5-38.

Jolley, S. J., H. Dijk, J. H. Lamens, Q. J. Fisher, T. Manzocchi, H. Eikmans and Y. Huang, 2007, Faulting and fault sealing in production simulation models: Brent Province, northern North Sea: Petroleum Geoscience, Vol. 13, pp. 1-20.

Katz, A. J. and A. H. Thompson, 1987, Prediction of rock electrical conductivity from mercury injection measurements: Journal of Geophysical Research B v. 92, # B1, p. 599-607.

Lickerish, H. and C. Tueckmantel, 2007, Normal Fault Zone Architecture: Gulf of Suez, Chapter 2.2, in: Davies, R. and R. Knipe, eds, Rock Deformation Research 2007 Project Review, Report 9536, p. 2.2-1-2.2-42.

Lickerish, H. and C. Tueckmantel, 2008, Mapped Fault Style Examples 2008: Examples from the Gulf of Suez, Chapter 2.3, in: Davies, R. and R. Knipe, eds., Rock Deformation Research Foundation Project 2008, Report 9582, p. 32-94.

Manzocchi, T., J. J. Walsh, P. Nell, and G. Yielding, 1999, Fault transmissibility multipliers for flow simulation models: Petroleum Geoscience, v. 5, p.53-63.

Solum, J. C., J. P. Brandenburg, et al., 2010, Characterization of deformation bands associated with normal and reverse stress states in the Navajo Sandstone, Utah: AAPG Bulletin, v. 94#9, p. 1453-1375.

Tueckmantel, C., Q. J. Fisher, R. J. Knipe, H. Lickerish, S. M. Khalil, 2010, Fault seal prediction of seismic-scale normal faults in porous sandstone: A case study from the eastern Gulf of Suez rift, Egypt: Marine and Petroleum Geology 27 (2010) 334-350.

Acknowledgements

This research was supported by the Rock Deformation Research Ltd. Fault Foundation Industrial Consortium sponsored by Anadarko, BG, BHP Billiton, BP, Chevron, Conoco-Phillips, Dong, Hess, Maersk, Petrobras, PetroChina, Shell, Statoil, Wintershall, and Woodside. Companies are thanked individually and collectively for their support. We also thank Rob Knipe, Michael Welch, Henry Lickerish, and Christian Tueckmantel for discussions about fault heterogeneity and fault-rock evolution, Plano Research Corporation is gratefully acknowledged for allowing use of the FlowSim reservoir simulator and associated visualization packages. This study would not have been possible without suitable modeling software. Dr. Anil Chopra and PetroTel Inc. are acknowledged for support of this research. I also thank Shekhar Jayanti of Petrotel, Inc. for help with simulation "nuts and bolts" issues.